

Article

Nitrogen Doped Carbon-Dot Embedded Poly(lactic acid-co-glycolic acid) Composite Films for Potential Use in Food Packing Industry and Wound Dressing

Mehtap Sahiner ¹, Betül Ari ², Manoj K. Ram ³ and Nurettin Sahiner ^{2,4,5,*}

¹ Bioengineering Department, Faculty of Engineering, Canakkale Onsekiz Mart University, Terzioğlu Campus, 17100 Canakkale, Turkey

² Department of Chemistry, Faculty of Sciences & Arts, and Nanoscience and Technology Research and Application Center (NANORAC), Canakkale Onsekiz Mart University, Terzioğlu Campus, 17100 Canakkale, Turkey

³ PolyMaterials APP. LLC, 3802 Spectrum Blvd, Suite 201, Tampa, FL 33612, USA

⁴ Department of Chemical, Biomedical Engineering, and Materials Science and Engineering, University of South Florida, Tampa, FL 33620, USA

⁵ Department of Ophthalmology, University of South Florida, Tampa, FL 33620, USA

* Correspondence: sahinert71@gmail.com

Abstract: Here, nitrogen-doped carbon dots (N-doped CDs) were synthesized by the hydrothermal method embedded within poly(lactic acid-co-glycolic acid) ((PLGA)) films at different amounts. The N-doped CDs (or CD) that possess fluorescence properties also have antimicrobial properties against *S. aureus* and *E. coli* microorganisms, determined by the disc diffusion method with 19 ± 2 and 18 ± 1 mm zone diameters, respectively. The CD embedded PLGA films (CD@PLGA) with different CD contents revealed an increased fluorescence intensity with the increased amount of CD. Moreover, the antibacterial potency of 50% CD containing PLGA (50-CD@PLGA) films (by weight) against *S. aureus* and *E. coli* microorganisms was examined and the zone diameters were found to be 14 ± 1 and 13 ± 1 mm, respectively. In addition, CD release studies from different amounts of CD (2.5–50 by weight) containing composite films showed that 50-CD@PLGA film released 127 ± 16 mg/g CD dots, which is $38 \pm 5\%$ of the embedded CDs in about 12 days, suggesting their potential application in food packing and wound dressing. Moreover, all CD@PLGA films were found to be blood compatible via hemolysis and blood clotting index tests with $<5\%$ hemolysis and $>90\%$ blood clotting indices regardless of their CD content.

Keywords: fluorescence film composite; carbon dot; antimicrobial film; hemocompatible; food packing; wound dressing



Citation: Sahiner, M.; Ari, B.; Ram, M.K.; Sahiner, N. Nitrogen Doped Carbon-Dot Embedded Poly(Lactic Acid-Co-Glycolic Acid) Composite Films for Potential Use in Food Packing Industry and Wound Dressing. *J. Compos. Sci.* **2022**, *6*, 260. <https://doi.org/10.3390/jcs6090260>

Academic Editor:
Francesco Tornabene

Received: 14 August 2022
Accepted: 6 September 2022
Published: 8 September 2022

Publisher's Note: MDPI stays neutral with regard to jurisdictional claims in published maps and institutional affiliations.



Copyright: © 2022 by the authors. Licensee MDPI, Basel, Switzerland. This article is an open access article distributed under the terms and conditions of the Creative Commons Attribution (CC BY) license (<https://creativecommons.org/licenses/by/4.0/>).

1. Introduction

Plastics have widespread use in food packaging due to their easy availability and cost effectiveness. However, plastics cause very serious environmental problems [1]. Environmentally friendly, biodegradable, and functional food packaging materials are gaining continuing importance. It is advantageous for food packaging to be able to detect deterioration and prevent spoilage. Microbial communities can be detected and identified with a wide range of application methodologies, such as Species-specific PCR [2], PCR-DGGE [3], and so on. Besides this, freshness indicators also exist that work via the sensory changes in food to detect toxicity, meat spoilage, and fruit ripening. However, most of the spoilage and microbial detectors are either expensive or non-mobile systems, and, as a result, the industry still requires easy synthesis, low cost, and fast detection methodologies. In addition, the presence of antimicrobial properties in food packaging increases the shelf-life of the food and food safety. There are studies on food packaging consisting of films containing nanoparticles, metal nanoparticles, essential oils, liposomes, or various phenolics [4]. In

the literature, a film was developed from sodium carboxymethyl cellulose and polyvinyl alcohol doped with anthocyanins that prepared an active and pH-responsive sensitivity to monitor the freshness of pork [5]. Active food packaging materials reported include sulfur-functionalized CDs embedded in pectin and gelatin films that have UV-barrier properties and antioxidant properties [1].

The skin is an organ that covers our body and protects it from the environment. Any wound on the skin needs to be protected from external microorganisms such as bacteria, viruses, and fungi. Moist and antimicrobial materials are very effective in the healing of wounds [6,7]. Three-dimensional hydrogel networks could be used to cure infected wounds [8]. Pharmaceuticals and drug delivery systems commonly utilize PLGA, a hydrophobic copolymer approved by the Food and Drug Administration (FDA, Silver Spring, MD, USA) [9]. In addition to its biocompatibility [10], biodegradability [11], and low toxicity [12], this polymer provides controlled drug delivery opportunities, as well as improved clinical experience.

In the last decade, the emergence of CDs, one of the carbon allotropes, has attracted intense interest due to its great capabilities and use in areas such as photocatalysis [13], and optoelectronic devices [14], due to its bio-imaging [15], biosensor [16], anti-bacterial [17], and anti-biofilm [18] properties. Besides these properties, its low toxicity, and great biocompatibility [19], and use in easy synthesis methodologies, such as laser ablation [20], hydrothermal treatment [21], and microwave and ultrasound methods [18], makes CDs one of the most promising advanced materials to detect food spoilage and act as a sensor due to their fluorescent and anti-bacterial properties.

In this study, CD embedded PLGA films were synthesized for use in food packing and wound dressing materials. Citric acid monohydrate (CA) was used as the carbon and polyethyleneimine (PEI) was used as a nitrogen source to create N-doped-CDs. It is known that amine functional groups contain structures that are further modifiable and make the material antibacterial. The N-doped-CDs used here are <100 nm in size and have fluorescent and biocompatible possessing antibiofilm, and antibacterial properties [22]. The CD@PLGA-composite films were fabricated by introducing CDs in PLGA solution at different amounts and casting into Petri dishes. The antibacterial properties of CD@PLGA-composite films against *S. aureus* and *E. coli* microorganisms was assessed as zone inhibition diameters. Furthermore, CD release studies from different amounts of CD@PLGA-composite films were investigated.

2. Materials and Methods

Citric acid (CA, Carlo Erba, >99%) as the carbon precursor and polyethyleneimine solution (PEI, 50 wt% in H₂O, Mn: 1800) as the nitrogen precursor were used to synthesize the N-doped CD. Poly(lactic acid-co-glycolic acid) (PLGA, Purasorb PLG-8531, Corbion, Amsterdam, The Netherlands) was used as a template for the film formation and chloroform (Riedel-de Haën, >99%) was used as a solvent for dissolving the PLGA. For the antimicrobial test, the Gram-positive microorganism *S. aureus* ATCC 6538 (KWIK-STIK™) and Gram-negative microorganism *E. coli* ATCC 8739 (KWIK-STIK™) bacterial strains were procured from Microbiologic. Nutrient agar and nutrient broth were purchased from Merck for the bacterial medium.

2.1. Synthesis of N-Doped CD and CD@PLGA Films

Primarily using citric acid (CA) as a carbon source and polyethyleneimine (PEI) as a nitrogen source, the N-doped CDs were prepared by applying some modifications to the hydrothermal method as reported in the literature [22,23]. A solution of 1.0 g of CA in 22 mL of water was prepared. Then, 6.0 mL of 50% aqueous PEI solution was added to the solution and stirred continuously for another 5 min. The mixed solution was transferred to a 50 mL capacity inner Teflon-lined reaction chamber. This reaction chamber was placed in a stainless-steel hydrothermal autoclave. This autoclave was placed in a furnace and kept at 250 °C for 4 h. N-doped CDs were synthesized hydrothermally in an inner Teflon-

lined autoclave at 250 °C for 4 h. The collected mixture was then moved to a dialysis membrane (molecular weight cut off 12,000 Da) and washed with distilled water for 24 h, with the water being refreshed every 8 h to get rid of unwanted organic molecules and for purification. Finally, rotary evaporation was used to concentrate the liquid N-doped CDs.

Following that, a 50 mg/mL PLGA solution in chloroform was prepared and stirred on a magnetic stirrer at 500 rpm for 2 h to dissolve the PLGA. In a separate vial, a 25 mg/mL N-doped CDs solution was prepared in chloroform. To prepare the N-doped CDs embedded films and illustrate the effects of the N-doped CDs numbers, different quantities of N-doped CDs (2.5–50 percent N-doped CDs by weight of PLGA) were added to the PLGA solution. Stirring was continued for 30 min to ensure that the N-doped CDs were uniformly and properly dispersed in the PLGA solution. The prepared film solutions were then poured into 90 mm diameter glass Petri dishes and left at room temperature for 24 h to form films.

2.2. Characterization of CD@PLGA Films

To determine the functional groups in the configuration of the film samples, a Fourier Transform Infrared Radiation Spectroscopic Analyzer (FT-IR, Perkin Elmer Spectrum 100, Akron, OH, USA) was used. The ATR technique was used to generate the FT-IR spectra with a wavenumber spectrum of 4000–650 cm^{-1} and a resolution of 4 cm^{-1} . Using a thermogravimetric analyzer (SII TG/DTA 6300, Seiko Instruments Inc., Chiba, Japan), the thermal activity of the prepared films was assessed. Then, nearly 3 mg of dry sample from the prepared films was placed into ceramic tubs. The thermal degradation of the samples in the N_2 (g) atmosphere at 100 mL/min flow rate, 10 °C/min heating rate, and 100–900 °C temperature range was investigated. A graph showing the temperature versus weight loss was created to represent the thermal degradation of the samples.

2.3. N-Doped CDs Released from CD@PLGA Film

N-doped CDs released from CD@PLGA films were investigated at PBS. Nearly 30 mg of dry film samples were weighed and placed in Falcon tubes containing 30 mL of PBS. These Falcon tubes were placed in a 37.5 °C water bath and stirred at 200 rpm. The composite film contained varying amounts of CDs. Measurements were taken at 437 nm and 550 PMT voltages in a fluorescence spectrometer using fluorescence spectroscopy (Lumina, Thermo Fisher Scientific, Waltham, MA, USA) at certain time intervals from the emission media containing the composite films containing different amounts of CD. A calibration curve was plotted for the N-doped CDs in PBS to calculate the released number of CDs.

2.4. Hemocompatibility of CD@PLGA Films

Depending on the field of use and the purpose of the materials that come into contact with blood, they should not cause blood coagulation and hemolysis in internal and external applications. With arterial and healthy human blood, hemocompatibility can easily and accurately be tested in vitro. The hemocompatibility assay of the CD@PLGA films was carried out by performing some modifications to the hemocompatibility tests reported in the literature [24]. Hemocompatibility studies were carried out with the approval of the ethics committee no. (KA EK-2011-KA EK-27/2022-2200063689), which was approved by the Human Research Ethics Committee of Çanakkale Onsekiz Mart University. Arterial blood was intravenously taken from healthy volunteers for the hemocompatibility tests. These blood samples were placed in blood tubes containing an anti-clotting agent, and the hemolysis and coagulation tests were started swiftly.

For the hemolysis test, dry samples weighing 10 mg were placed in 9.8 mL of 9% physiological saline solution. Then, a 2:2.5 by volume of blood and 9% physiological saline solution were mixed and gently shaken. Subsequently, 0.2 mL of this blood was transferred to the tubes containing the sample. It was kept at 37.5 °C for 2 h to incubate. Water was used as a positive control and physiological saline solution as a negative control, which were tested by simultaneous exposure to the same conditions.

After the incubated solutions were centrifuged at 1340 rpm for 5 min, the absorbance of the supernatant solution was determined using a UV-Vis Spectrophotometer at a 542 nm wavelength. The hemolysis index% of the samples was calculated according to the formula in Equation (1).

$$\text{Hemolysis Index\%} = \left(A_{\text{sample}} - A_{\text{saline}} \right) / \left(A_{\text{water}} - A_{\text{saline}} \right) \times 100 \quad (1)$$

For the blood coagulation test, pieces of film weighing about 10 mg were placed in a centrifuge tube. In another tube, 0.064 mL of 0.2 M CaCl₂ solution was added to 0.81 mL of arterial blood, and 0.27 mL was taken from this blood solution and brought into contact with the samples. Then, the tubes were incubated at 37.5 °C for 10 min. After incubation, 10 mL of DI water, kept at 37.5 °C, was slowly added to the blood-containing samples and centrifuged for 1 min at 540 rpm. The liquid part in the tube was then added to 40 mL of DI water, kept at 37.5 °C, and incubated for 2 h at 37.5 °C. As a control, 0.25 mL of blood was added to 50 mL of DI water, kept at 37.5 °C, and incubated for 1 h under the same conditions. The absorbance of the incubated solutions was determined at a 542 nm wavelength using a UV-vis Spectrophotometer. The blood coagulation index% of the samples was calculated using Equation (2).

$$\text{Blood coagulation Index\%} = \left(A_{\text{sample}} / A_{\text{control}} \right) \times 100 \quad (2)$$

2.5. Antibacterial Activity of CD@PLGA Films

The antimicrobial properties of the prepared CD@PLGA films were determined by the disc diffusion method against Gram-negative *E. coli* and Gram-positive *S. aureus* bacterial strains. The films and N-doped CDs whose antimicrobial effects were to be examined were kept under 420 nm UV light for 1 min for sterilization. Briefly, for the antimicrobial test, the stock microorganism suspension was adjusted to a concentration of approximately 0.5×10^8 CFU/mL (colony forming units) according to the McFarland 0.5 standard, and 0.1 mL of this suspension was inoculated on a nutrient agar plate. Three pieces of sterile discs with a diameter of 9 mm were placed on the plate, and immediately 10 µL, 20 µL, and 30 µL of 100 mg/mL concentration of the N-doped CDs suspension in 0.9% NaCl saline solution were dropped onto these discs. Moreover, 10 × 10 mm sized PLGA and CD@PLGA films were placed onto another plate and these plates were incubated at 35 °C for 24 h. After this process, the clear zone around the discs was measured in mm to determine the inhibition zone of the materials against the bacteria.

3. Results

3.1. Preparation and Characterization of CD@PLGA Film

N-doped CDs were synthesized using the hydrothermal method, the best known and frequently used method for CD synthesis, using CA as the carbon source and PEI as the nitrogen source. The characterization of the N-doped CDs was given in our previous study. As shown schematically in Figure 1a, the solution prepared using CA:PEI in a ratio of 1:1 by weight was reacted in a furnace at 250 °C for 4 h to form the N-doped CDs. The N-doped CDs removed from the furnace at the end of the reaction were cooled to room temperature and the resulting yellowish-brown liquid was transferred to the dialysis membrane. It was then washed for 24 h with the water refreshed every 8 h to get rid of unwanted organic molecules. Then, the N-doped CDs were dispersed in chloroform at a concentration of 25 mg/mL. PLGA at a concentration of 50 mg/mL in another vial was dissolved in chloroform for 2 h. After this, the N-doped CDs dispersed in chloroform were incorporated into the PLGA film structure as shown in Figure 1b and mixed for 30 min to ensure that the N-doped CDs were evenly distributed in the PLGA film solution. Then, the CD@PLGA was kept at room temperature for 24 h for film formation.

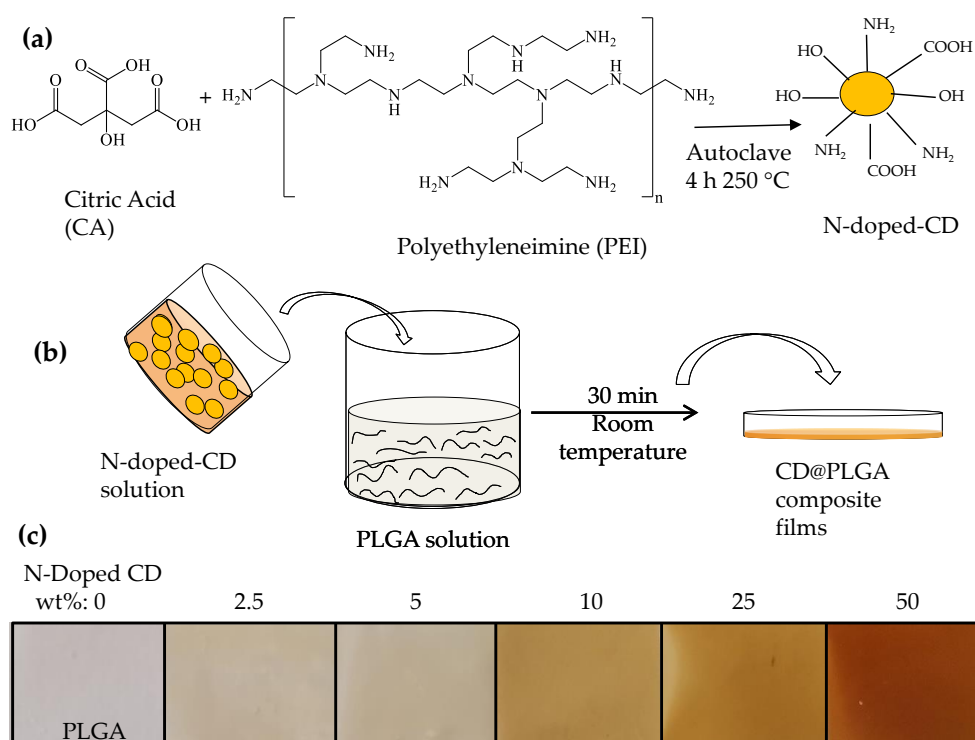


Figure 1. Schematic representation of the synthesis of (a) N-doped CD; (b) CD@PLGA composite film preparation; and (c) digital camera images of the corresponding films.

In Figure 1c, digital camera images of the films containing N-doped CDs in the ratios of 0, 2.5, 5, 10, 25 and 50% by the weight of the PLGA are given. As can be seen from the digital camera images, the images close to being transparent become darker with the increase in the number of N-doped CDs contained in the films.

FT-IR spectroscopy was used to verify the surface functional groups of the synthesized N-doped CDs and films. The FT-IR spectra given in Figure 2a have been attributed to the stretching vibration associated with the peak C=O ester group at 1750 cm^{-1} [25]. As can be clearly seen from the FT-IR spectrum, the 2.5-CD@PLGA, 5-CD@PLGA, and 10-CD@PLGA films show the same characteristic peaks as the PLGA film. This can be explained by the fact that PLGA contains fewer numbers of N-doped CDs relative to its weight and the results are not shown in the FT-IR spectra. On the other hand, the wideband observed between $3281\text{--}3272 \text{ cm}^{-1}$ observed in the 25-CD@PLGA, and 50-CD@PLGA films ascribe the presence of -OH and N-H, which is characteristic of N-doped CDs. In addition, the characteristic N-doped CDs peaks are attributed to the C-N stretch at 1555 cm^{-1} and the N-H bending vibrations at 1656 cm^{-1} [26–28].

The thermograms of the TG analysis results were performed on films under N_2 (g), at a 100 mL/min flow rate, and a constant heating rate of $10 \text{ }^\circ\text{C}/\text{min}$ for 25–100 $^\circ\text{C}$ to remove the moisture. Then, the temperature rose between 100–900 $^\circ\text{C}$ as demonstrated in Figure 2b. According to the thermograms shown in Figure 2b, the 2.5-CD@PLGA, 5-CD@PLGA, and 10-CD@PLGA films degrade in one stage, and the 25-CD@PLGA and 50-CD@PLGA films degrade in three stages. The thermograms of PLGA and the 2.5-CD@PLGA, 5-CD@PLGA, and 10-CD@PLGA films are similar. These films show a weight loss of about 96% between 275–390 $^\circ\text{C}$. When the temperature reaches 900 $^\circ\text{C}$, the final weight loss is almost 98%. The 25-CD@PLGA film degraded in three stages and exhibited a weight loss of 73% in the 190–290 $^\circ\text{C}$ temperature range, 85% in the 300–420 $^\circ\text{C}$ temperature range, and 87% in the 420–900 $^\circ\text{C}$ temperature range. The 50-CD@PLGA film was also degraded in three stages. The first stage started at 190 $^\circ\text{C}$ and ended at 280 $^\circ\text{C}$, which corresponds to a weight loss of almost 67%. The second stage of degradation started at 280 $^\circ\text{C}$ and ended with a weight

loss of 90% at 420 °C. The final stage of degradation started at 420 °C and continued up to 900 °C, and this stage ended with a weight loss of about 96%.

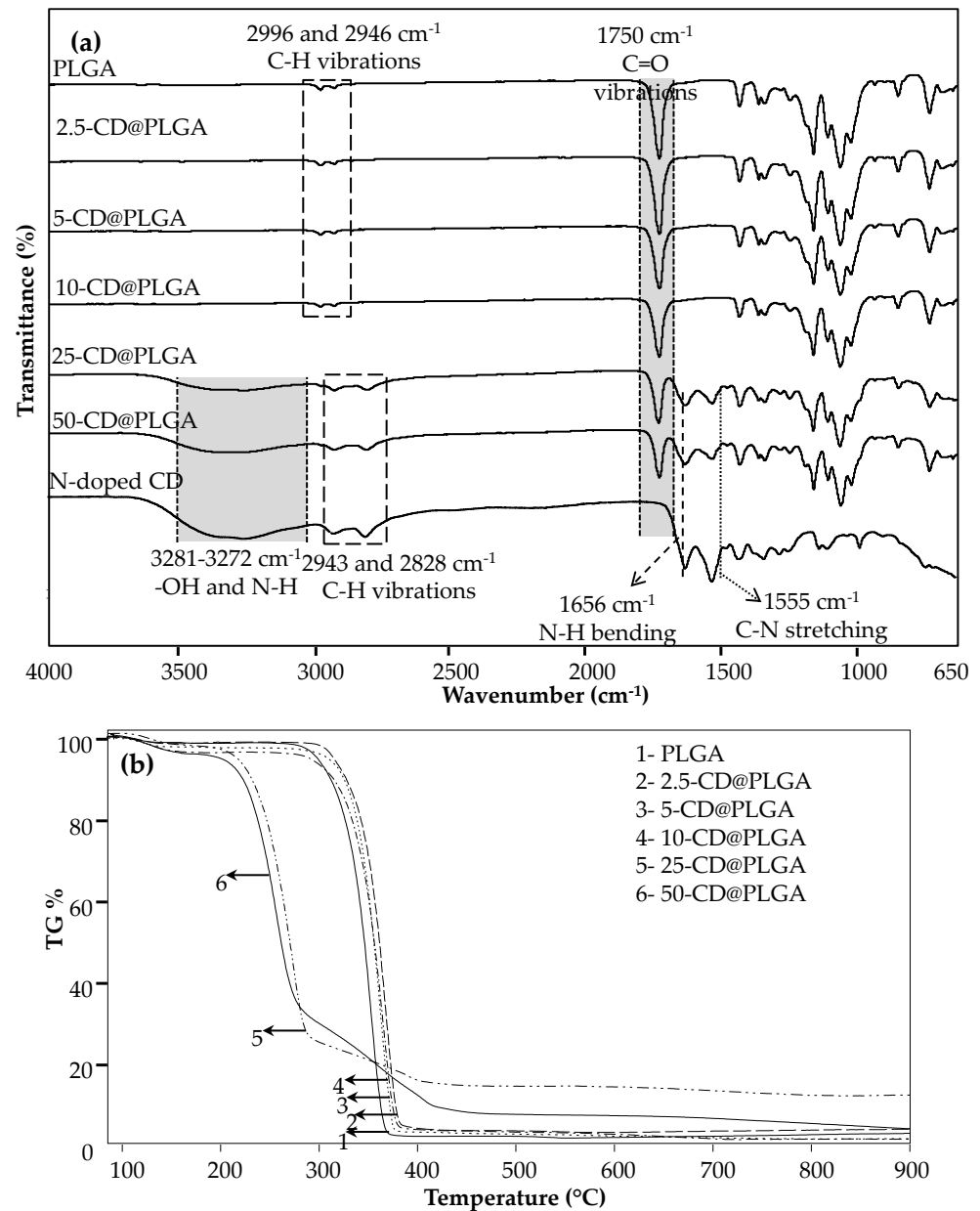


Figure 2. (a) FT-IR spectra of N-doped CD and CD@PLGA with different CD contents, and (b) their corresponding thermograms.

3.2. N-Doped CDs Released from CD@PLGA Films

N-doped CDs were synthesized by the hydrothermal method and embedded into the PLGA films in different amounts. The release rate was determined by the degradation of the films via Fluorescence Spectrum at pH 7.4. According to the results given in Figure 3a, all films release N-doped CDs, almost linearly, for up to about 24 h, and the N-doped CDs release continues slowly up to a period of 14 days until a plateau is reached. The N-doped CDs release amounts were 0.05 ± 0.01 , 0.07 ± 0.01 , 2.2 ± 0.1 , 31.2 ± 6.1 and 124.2 ± 9.1 mg/g after 10 days for the 2.5-CD@PLGA, 5-CD@PLGA, 10-CD@PLGA, 25-CD@PLGA and 50-CD@PLGA films, respectively. In addition, the cumulative N-doped CDs release percentages of the films were calculated, and the results are given in Figure 3b. The cumulative N-doped CDs released from the films varied from $0.5 \pm 0.04\%$ to $38 \pm 5\%$

depending upon the number of N-doped CDs they involved. The Figure 3b inset shows the digital camera images under daylight and the UV light illumination of the samples withdrawn from the PBS release medium. It was observed that the images were transparent under daylight and only the 10-CD@PLGA, 25-CD@PLGA and 50-CD@PLGA films exhibited a bright blue, fluorescent color at 366 nm UV light illumination. With the increasing numbers of N-doped CDs in these films, the bright blue color intensity increases. The fact that the 2.5-CD@PLGA and 5-CD@PLGA films lack fluorescence features is explained by their low N-doped CDs content. What is more, these data for each film sample were fortified by their fluorescence spectrum as demonstrated in Figure 3c. The 2.5-CD@PLGA, 5-CD@PLGA, 10-CD@PLGA, 25-CD@PLGA, and 50-CD@PLGA films have characteristic peaks at 412, 412, 434, 437, 437 and 437 nm, respectively. However, the fluorescence spectra of the films containing different amounts of N-doped CDs indicate that, as the number of N-doped CDs in the CD@PLGA films increased, a gradual increase in the fluorescence intensity of the samples was observed.

As can clearly be seen from Figure 3, the differences between the release rate of N-doped CDs are related to the films, including the different amounts of N-doped CDs. In conclusion, as the rate of the number of N-doped CDs in the films increased, the amount of the N-doped CDs release, percentage, and fluorescence spectrum also increased linearly as illustrated in Figure 3a–c, respectively. The results showed that the number of N-doped CDs released, the cumulative release rate, and the fluorescence property was notably affected by the number of N-doped CDs the films contained.

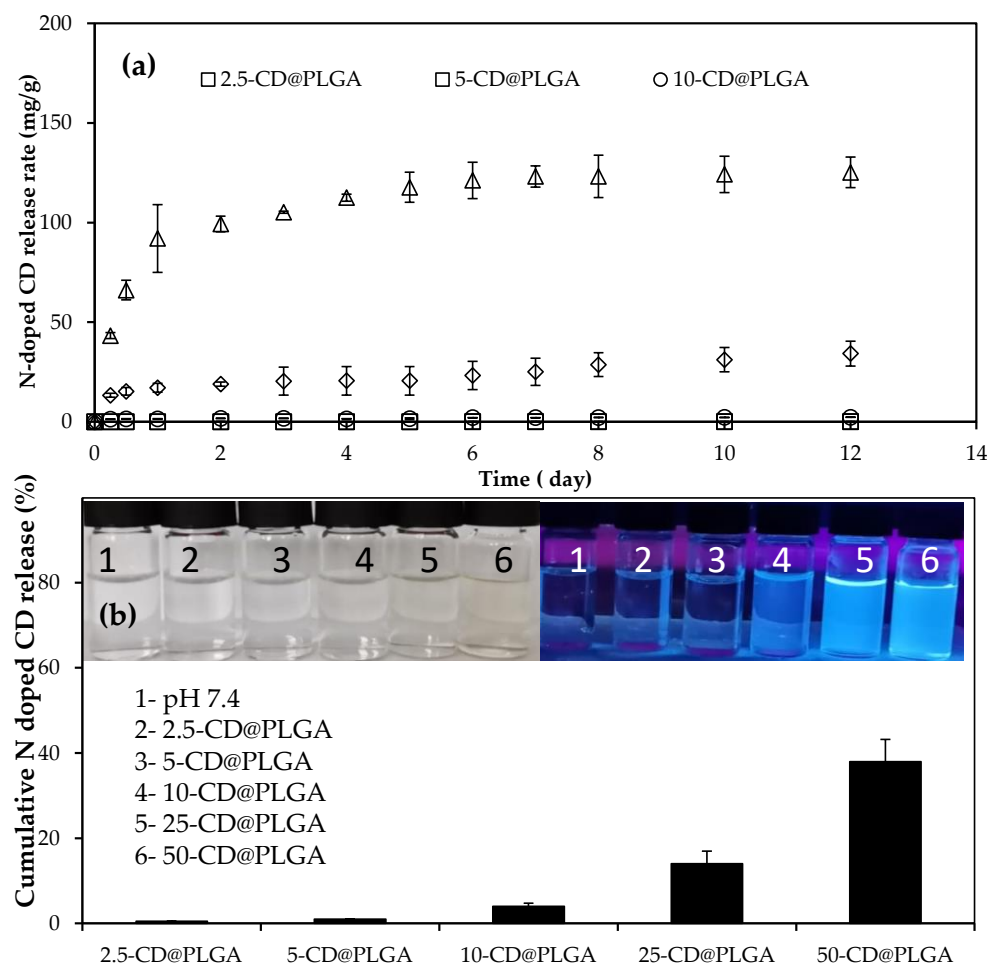


Figure 3. Cont.

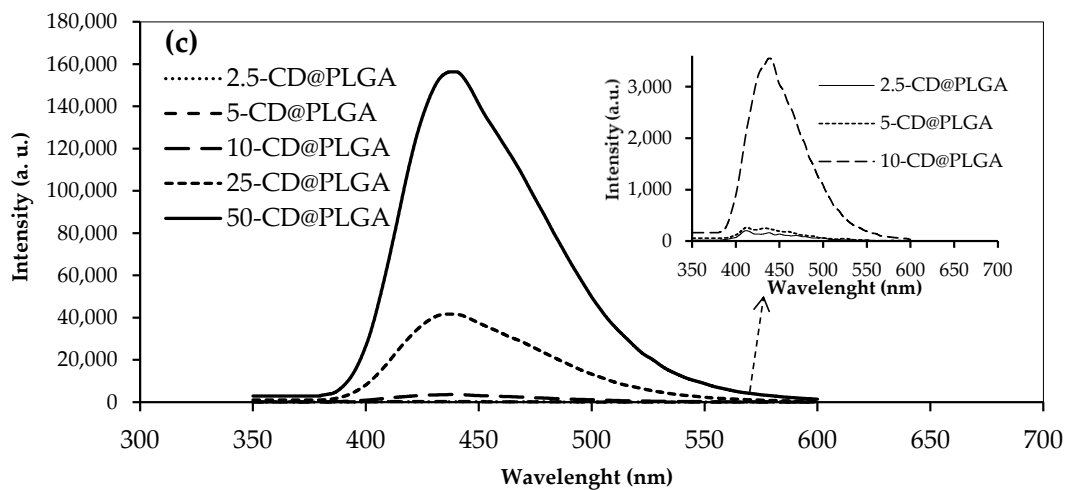


Figure 3. (a) The N-doped CD release (mg/g) from CD@PLGA containing different amounts of CDs; (b) cumulative release (%); and (c) fluorescence emission spectra of films [Reaction conditions: 30 mg film, 30 mL pH 7.4 solution, 37.5 °C, 200 rpm mixing rate].

3.3. Hemocompatibility Test Results of CD@PLGA Films

Material hemocompatibility is one of the parameters to consider in biological applications. Hemolysis and blood coagulation tests were conducted to assess the potential use of 10 mg PLGA films in the blood-contact application. Figure 4 shows the hemocompatibility results of films with in vitro hemolysis and blood coagulation tests. According to the hemolysis index results given in Figure 4a, all CD@PLGA and PLGA films are non-hemolytic.

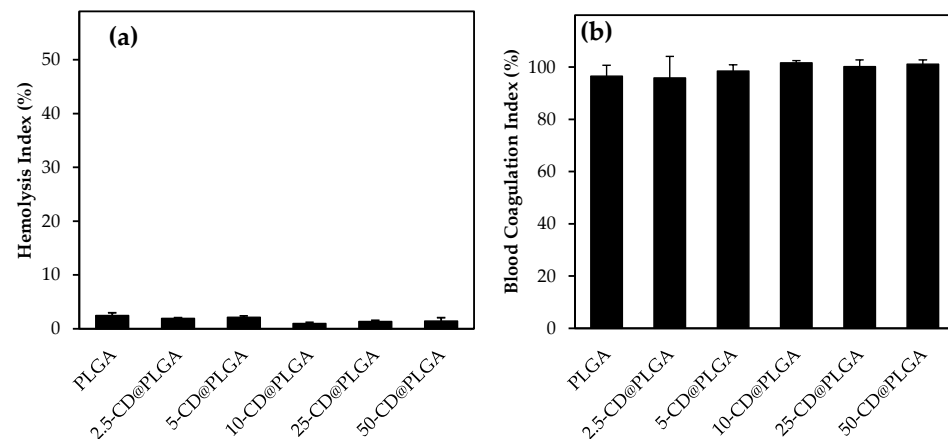


Figure 4. Hemocompatibility of 10 mg PLGA and CD@PLGA films via (a) hemolysis, and (b) blood coagulation tests.

Figure 4b exhibits the blood coagulation index results of the films. As can be seen from the results, the film blood coagulation index ranges from $97 \pm 4\%$ to $100 \pm 2\%$ for PLGA and CD@PLGA films.

As a result, irrespective of the number of N-doped CDs it contains, all films are hemocompatible and can be utilized confidently in studies that come into contact with blood.

3.4. Antimicrobial Activity of CD@PLGA Films

The antibacterial effect of N-doped CDs, PLGA, and CD@PLGA films against *S. aureus* and *E. coli* microorganisms was tested via the disc diffusion method. Digital camera images of the inhibition zone against both types of microorganisms are illustrated in Figure 5

and the results are summarized in Table 1. As can be clearly seen from the digital camera images, the zone diameter could be measured for all samples except for the PLGA film. For the different concentrations of N-doped CDs, the sample zone diameters increased with the increasing N-doped CDs concentration. The antibacterial effect of the N-doped CDs was investigated using CD at three different concentrations: 1 mg/mL, 2 mg/mL, and 3 mg/mL. Likewise, the zone diameters of the PLGA and 50-CD@PLGA films are given in Figure 5. The inhibition zone of the PLGA film was not observed against both microorganisms, but the inhibition zone of the 50-CD@PLGA film was easily measured.

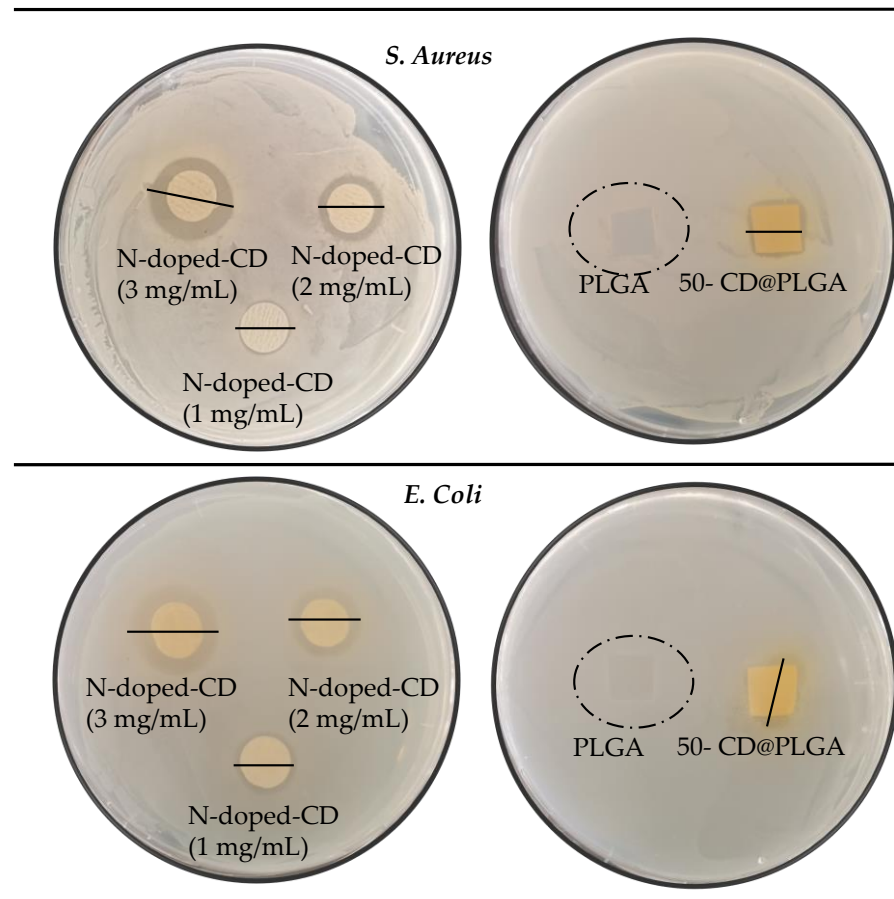


Figure 5. Digital camera images of the zone inhibition diameters on *S. aureus* and *E. coli* according to the disc diffusion method for N-doped-CD, PLGA, and 50-CD@PLGA.

Table 1. Inhibition zone diameter of N-doped CDs and 50-CD@PLGA films against *S. aureus* and *E. coli*.

Materials	Inhibition Zone (mm)	
	<i>S. aureus</i> (Gram Positive)	<i>E. coli</i> (Gram Negative)
N-doped-CD (1 mg/mL)	12 ± 1	12 ± 1
N-doped-CD (2 mg/mL)	15 ± 1	14 ± 1
N-doped-CD (3 mg/mL)	19 ± 2	18 ± 1
PLGA	-	-
50-CD@PLGA	13 ± 1	12 ± 1

As given in Table 1, the inhibition zone diameters of the N-doped CDs, for the concentration of 1, 2 and 3 mg/mL against *S. aureus* were measured as 12 ± 1, 15 ± 1 and 19 ± 2 mm, respectively. When the same concentrations of N-doped CDs were

analyzed against *E. coli*, the zone diameters were determined as 12 ± 1 , 14 ± 1 and 18 ± 1 mm, respectively.

The inhibition zone diameters of the PLGA and 50-CD@PLGA films are also given in Table 1. Although the PLGA film did not show any zone diameter against *S. aureus* and *E. coli*, the 50-CD@PLGA film reached a 13 ± 1 mm zone diameter against *S. aureus* and a 12 ± 1 mm zone diameter against *E. coli*. As 50-CD@PLGA films contain high amounts of N-doped CDs, the release of N-doped CDs in the *S. aureus* and *E. coli* media are limited, and therefore, the zone diameter may not have been revealed very clearly. However, given enough time and an aqueous environment, the degradation of the PLGA matrix will enable higher amounts of N-doped CDs that are very effective in killing *S. aureus* and *E. coli* microorganisms.

4. Conclusions

N-doped CDs were successfully synthesized via a hydrothermal method using CA:PEI at a ratio of 1:1 by weight as the precursors. The N-doped CDs were embedded in the PLGA films at different ratios and their controllable release behavior was investigated using fluorescence spectroscopy due to the fluorescence properties of the CDs. The results support how the release behavior could be controlled by increasing the number of CDs within the CD@PLGA film composites. Likewise, the antimicrobial effect of the films has also revealed a distinct result between films with and without CDs. Although no zone inhibition diameter is seen in PLGA films, the antibacterial activity of the 50-CD@PLGA film against *S. aureus* and *E. coli* bacterial strains has been revealed with zone inhibition diameters of 14 ± 1 and 13 ± 1 mm, respectively. In brief, CD@PLGA films can be used safely in fields such as food packaging products, medicine, and biomedicine as sensors with antimicrobial and fluorescent properties.

Attaining safe food with long-lasting storage capacity is very important for human health due to socio-economic considerations and income irregularity. Various strategies need to be adopted, including the use of smart packing materials. For example, to increase the shelf-life of meat products, antioxidants and/or antimicrobials in different formulations, whether synthetic or natural, must be used as additives. Food additives and/or smart food packing materials could be used to extend the shelf-life of foods, e.g., meat and meat products to prevent microbial spoilage [26]. It is important to note that many of the additives used in food processing plants can cause carcinogenic effects, food allergies, toxicity, or sensitivities [25]. In this regard, it is crucial to monitor food freshness and spoilage to ensure food safety and quality by employing smart packing materials that can prevent spoilage and signal decay, such as the one reported here, namely CD@PLGA composite films.

Author Contributions: Conceptualization, N.S.; methodology, M.S. and B.A.; software, M.S.; validation, M.S. and B.A.; formal analysis, M.S., B.A. and M.K.R.; investigation, M.S. and B.A.; resources, N.S.; data curation, M.S., B.A. and M.K.R.; writing—original draft preparation, M.S., B.A. and M.K.R.; writing—review and editing, N.S.; visualization, N.S.; supervision, N.S.; project administration, N.S.; funding acquisition, N.S. All authors have read and agreed to the published version of the manuscript.

Funding: This research received no external funding.

Informed Consent Statement: Not applicable.

Data Availability Statement: The data supporting the findings of this study are available within the article or upon request to the corresponding author.

Acknowledgments: The authors are grateful to Selin Sagbas Suner and Sahin Demirci for the help with some of the antibacterial studies and characterization of the materials.

Conflicts of Interest: The authors declare no conflict of interest.

References

1. Ezati, P.; Roy, S.; Rhim, J.-W. Pectin/gelatin-based bioactive composite films reinforced with sulfur functionalized carbon dots. *Colloids Surf. A Physicochem. Eng. Asp.* **2022**, *636*, 128123. [[CrossRef](#)]
2. Barakat, R.; Griffiths, M.; Harris, L. Isolation and characterization of Carnobacterium, Lactococcus, and Enterococcus spp. from cooked, modified atmosphere packaged, refrigerated, poultry meat. *Int. J. Food Microbiol.* **2000**, *62*, 83–94. [[CrossRef](#)]
3. Audenaert, K.; D'Haene, K.; Messens, K.; Ruysen, T.; Vandamme, P.; Huys, G. Diversity of lactic acid bacteria from modified atmosphere packaged sliced cooked meat products at sell-by date assessed by PCR-denaturing gradient gel electrophoresis. *Food Microbiol.* **2010**, *27*, 12–18. [[CrossRef](#)] [[PubMed](#)]
4. Machado, É.F.; Favarin, F.R.; Ourique, A.F. The use of nanostructured films in the development of packaging for meat and meat products: A brief review of the literature. *Food Chem. Adv.* **2022**, *1*, 100050. [[CrossRef](#)]
5. Wang, Y.; Zhang, J.; Zhang, L. An active and pH-responsive film developed by sodium carboxymethyl cellulose/polyvinyl alcohol doped with rose anthocyanin extracts. *Food Chem.* **2022**, *373*, 131367. [[CrossRef](#)]
6. Šnejdrová, E.; Martiška, J.; Loskot, J.; Paraskevopoulos, G.; Kováčik, A.; Regdon, G., Jr.; Budai-Szűcs, M.; Palát, K.; Konečná, K. PLGA based film forming systems for superficial fungal infections treatment. *Eur. J. Pharm. Sci.* **2021**, *163*, 105855. [[CrossRef](#)]
7. Liu, L.; Shi, J.; Sun, X.; Zhang, Y.; Qin, J.; Peng, S.; Xu, J.; Song, L.; Zhang, Y. Thermo-responsive hydrogel-supported antibacterial material with persistent photocatalytic activity for continuous sterilization and wound healing. *Compos. Part B Eng.* **2022**, *229*, 109459. [[CrossRef](#)]
8. Ahmadian, Z.; Gheybi, H.; Adeli, M. Efficient wound healing by antibacterial property: Advances and trends of hydrogels, hydrogel-metal NP composites and photothermal therapy platforms. *J. Drug Deliv. Sci. Technol.* **2022**, *73*, 103458. [[CrossRef](#)]
9. Mohebbi, A.; Abdouss, M. Layered biocompatible pH-responsive antibacterial composite film based on HNT/PLGA/chitosan for controlled release of minocycline as burn wound dressing. *Int. J. Biol. Macromol.* **2020**, *164*, 4193–4204. [[CrossRef](#)]
10. Li, D.; Sun, H.; Jiang, L.; Zhang, K.; Liu, W.; Zhu, Y.; Fangteng, J.; Shi, C.; Zhao, L.; Sun, H.; et al. Enhanced Biocompatibility of PLGA Nanofibers with Gelatin/Nano-Hydroxyapatite Bone Biomimetics Incorporation. *ACS Appl. Mater. Interfaces* **2014**, *6*, 9402–9410. [[CrossRef](#)]
11. Anderson, J.M.; Shive, M.S. Biodegradation and biocompatibility of PLA and PLGA microspheres. *Adv. Drug Deliv. Rev.* **2012**, *64*, 72–82. [[CrossRef](#)]
12. Fattal, E.; Mura, S.; Nicolas, J.; Hillaireau, H.; Gueutin, C.; Le Droumaguet, B.; Zanna, S.; Tsapis, N. Influence of surface charge on the potential toxicity of PLGA nanoparticles towards Calu-3 cells. *Int. J. Nanomed.* **2011**, *6*, 2591–2605. [[CrossRef](#)] [[PubMed](#)]
13. Fernando, K.A.S.; Sahu, S.; Liu, Y.; Lewis, W.K.; Gulians, E.A.; Jafariyan, A.; Wang, P.; Bunker, C.E.; Sun, Y.-P. Carbon Quantum Dots and Applications in Photocatalytic Energy Conversion. *ACS Appl. Mater. Interfaces* **2015**, *7*, 8363–8376. [[CrossRef](#)]
14. Li, X.; Rui, M.; Song, J.; Shen, Z.; Zeng, H. Carbon and Graphene Quantum Dots for Optoelectronic and Energy Devices: A Review. *Adv. Funct. Mater.* **2015**, *25*, 4929–4947. [[CrossRef](#)]
15. Luo, P.G.; Sahu, S.; Yang, S.-T.; Sonkar, S.K.; Wang, J.; Wang, H.; LeCroy, G.E.; Cao, L.; Sun, Y.-P. Carbon “quantum” dots for optical bioimaging. *J. Mater. Chem. B* **2013**, *1*, 2116–2127. [[CrossRef](#)]
16. Bui, T.T.; Park, S.-Y. A carbon dot–hemoglobin complex-based biosensor for cholesterol detection. *Green Chem.* **2016**, *18*, 4245–4253. [[CrossRef](#)]
17. Suner, S.S.; Sahiner, M.; Ayyala, R.S.; Bhethanabotla, V.R.; Sahiner, N. Nitrogen-Doped Arginine Carbon Dots and Its Metal Nanoparticle Composites as Antibacterial Agent. *C J. Carbon Res.* **2020**, *6*, 58. [[CrossRef](#)]
18. Suner, S.S.; Sahiner, M.; Ayyala, R.S.; Bhethanabotla, V.R.; Sahiner, N. Versatile Fluorescent Carbon Dots from Citric Acid and Cysteine with Antimicrobial, Anti-biofilm, Antioxidant, and AChE Enzyme Inhibition Capabilities. *J. Fluoresc.* **2021**, *31*, 1705–1717. [[CrossRef](#)]
19. Huang, Y.; Liang, Y.; Rao, Y.; Zhu, D.; Cao, J.; Shen, Z.; Ho, W.; Lee, S.C. Environment-Friendly Carbon Quantum Dots/ZnFe 2 O 4 Photocatalysts: Characterization, Biocompatibility, and Mechanisms for NO Removal. *Environ. Sci. Technol.* **2017**, *51*, 2924–2933. [[CrossRef](#)]
20. Calabro, R.L.; Yang, D.-S.; Kim, D.Y. Liquid-phase laser ablation synthesis of graphene quantum dots from carbon nano-onions: Comparison with chemical oxidation. *J. Colloid Interface Sci.* **2018**, *527*, 132–140. [[CrossRef](#)]
21. Sutekin, S.D.; Sahiner, M.; Suner, S.S.; Demirci, S.; Güven, O.; Sahiner, N. Poly(Vinylamine) Derived N-Doped C-Dots with Antimicrobial and Antibiofilm Activities. *C J. Carbon Res.* **2021**, *7*, 40. [[CrossRef](#)]
22. Abraham, W.L.; Demirci, S.; Wypyski, M.S.; Ayyala, R.S.; Bhethanabotla, V.R.; Lawson, L.B.; Sahiner, N. Biofilm inhibition and bacterial eradication by C-dots derived from polyethyleneimine-citric acid. *Colloids Surf. B Biointerfaces* **2022**, *217*, 112704. [[CrossRef](#)]
23. Wang, C.; Xu, Z.; Zhang, C. Polyethyleneimine-Functionalized Fluorescent Carbon Dots: Water Stability, pH Sensing, and Cellular Imaging. *Chem. Nanomater.* **2015**, *1*, 122–127. [[CrossRef](#)]
24. Sahiner, M.; Blake, D.A.; Fullerton, M.L.; Suner, S.S.; Sunol, A.K.; Sahiner, N. Enhancement of biocompatibility and carbohydrate absorption control potential of rosmarinic acid through crosslinking into microparticles. *Int. J. Biol. Macromol.* **2019**, *137*, 836–843. [[CrossRef](#)]
25. Singh, R.; Kesharwani, P.; Mehra, N.K.; Singh, S.; Banerjee, S.; Jain, N.K. Development and characterization of folate anchored Saquinavir entrapped PLGA nanoparticles for anti-tumor activity. *Drug Dev. Ind. Pharm.* **2015**, *41*, 1888–1901. [[CrossRef](#)] [[PubMed](#)]

26. Liu, C.; Zhang, P.; Zhai, X.; Tian, F.; Li, W.; Yang, J.; Liu, Y.; Wang, H.; Wang, W.; Liu, W. Nano-carrier for gene delivery and bioimaging based on carbon dots with PEI-passivation enhanced fluorescence. *Biomaterials* **2012**, *33*, 3604–3613. [[CrossRef](#)] [[PubMed](#)]
27. Han, S.; Chen, X.; Hu, Y.; Han, L. Solid-state N, P-doped carbon dots conquer aggregation-caused fluorescence quenching and couple with europium metal-organic frameworks toward white light-emitting diodes. *Dyes Pigment* **2021**, *187*, 109090. [[CrossRef](#)]
28. Liu, J.; Liu, X.; Luo, H.; Gao, Y. One-step preparation of nitrogen-doped and surface-passivated carbon quantum dots with high quantum yield and excellent optical properties. *RSC Adv.* **2014**, *4*, 7648. [[CrossRef](#)]